

# Stiffness methods for compaction control: the P-FWD device

Les méthodes de rigidité pour le contrôle du compactage : le deflectomètre à masse tombante (P-FWD)

M. C. Conde

*Instituto Superior de Engenharia de Lisboa, Lisbon, Portugal*

M. G. Lopes

*Instituto Superior de Engenharia de Lisboa, Lisbon, Portugal*

L. Caldeira

*Laboratório Nacional de Engenharia Civil, Lisbon, Portugal*

## ABSTRACT

Soil compaction is essential in the construction of highways, airports, buildings, bridges and dams. There is a current trend towards measuring the soil modulus instead the density. This approach is supported by the concept that the performance requirements (e.g., maximum soil strength, minimum permeability or minimum compressibility) may not correspond to the maximum soil dry density at its optimum water content.

This study was undertaken to show the feasibility of employing the portable falling weight deflectometer (P-FWD), with Prima 100 device, in order to estimate *in situ* stiffness modulus of soils and to demonstrate the correlation between the output of the Prima 100 device and water contents and compaction degrees.

## RÉSUMÉ

Le compactage des sols est essentiel dans la construction des autoroutes, des aéroports, des bâtiments, des ponts et des barrages. Il ya une tendance actuelle de mesurer la raideur au lieu de la densité. Cette approche est soutenue par l'idée que les exigences de performance (par exemple, la capacité portante maximale, la perméabilité minimum ou la compressibilité minimum du sol) peuvent ne pas correspondre à la teneur en eau optimale pour une densité sèche maximum du sol.

Cette étude a été entreprise afin de démontrer la faisabilité de l'utilisation du deflectomètre à masse tombante (100 Prima), afin d'évaluer *in situ* la raideur du sol et de démontrer la corrélation entre les résultats obtenus avec le deflectomètre portable à masse tombante (P-FWD), la teneur en eau et le degré de compactage.

Keywords :soil compaction, portable falling weight deflectometer, dynamic analysis, stiffness modulus

## 1 INTRODUCTION

Soil compaction is essential in the construction of highways, airports, buildings, bridges and dams. Typically compaction is controlled by measuring the dry density and the water content of the compacted soil and checking that target values have been achieved. There is a current trend towards measuring the soil stiffness modulus instead the density. This approach, especially in transportation infrastructures, is supported by the concept that the performance requirements (e.g., maximum soil strength and minimum compressibility) may not correspond to the maximum soil dry density at its optimum water content. But the use of stiffness measurement for control introduces the difficulty that these properties are very much dependent on both water content and density.

A comprehensive experimental testing program is under development in an effort to correlate the readings of three soil compaction control devices, based on stiffness methods (geogauge, light dynamic cone penetrometer and portable falling weight deflectometer), to soil dry density and water content, measured by nuclear and traditional methods (sand cone density and microwave oven heating tests, respectively).

The first objective of this paper is to show the feasibility of employing the portable falling weight deflectometer (P-FWD), with Prima 100 device, in order to estimate *in situ* soil stiffness modulus.

The second objective is to illustrate the correlation between the output of the Prima 100 device and water contents and compaction degrees.

## 2 EXPERIMENTAL WORK

With the objective of determining soil *in situ* stiffness modulus of a dam under construction, 11 test points on the upstream shell and 6 tests points on the downstream shell were selected. Since the modulus is dependent on unit weight and water content of the soil, these properties were also determined in-place by nuclear moisture-density tests and sand cone density tests.

Soil samples from each test point were collected in the same general area as the field test locations and stored to further laboratory characterization.

### 2.1 Laboratory study

Laboratory tests included index tests and Proctor compaction tests. Table 1 presents a summary of index and compaction results.

Table 1. Index and compaction tests results

Location	Max dry density (kN/m <sup>3</sup> )	Optimum water content (%)	w <sub>L</sub> (%)	PI (%)	AASHTO Classif.
Upstream and downstream shells	18.42	14.8	16	17	A-6 (8)

2.2 Field Study

Figure 1 presents a summary of field tests performed at each location and Figure 2 presents the different points location.

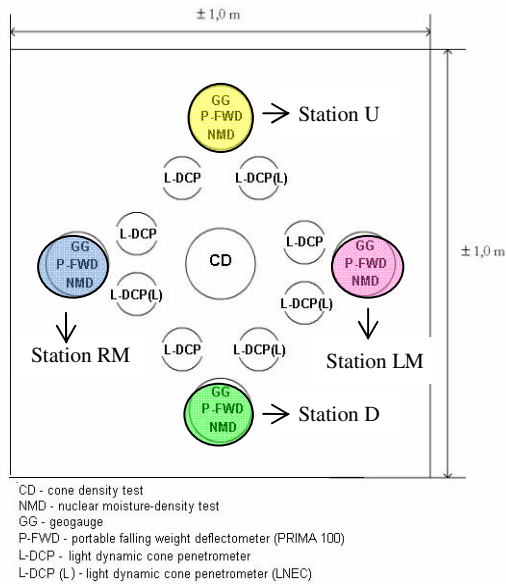


Figure 1. Field tests performed at each location.

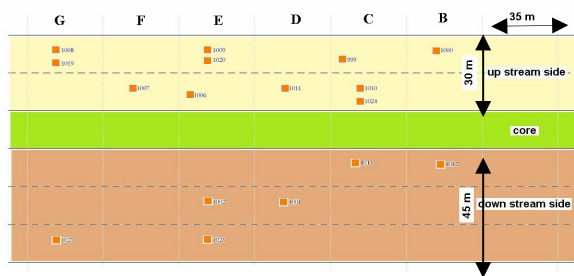


Figure 2. Different points location.

2.2.1 In-place Density and Water Content Tests

At every station of each test point, in the same location that the stiffness measurements were performed, dry density and water content data were determined by nuclear gauge. These results were compared with those obtained by traditional methods (by sand cone density and microwave oven heating tests, according to ASTM D 1556 and ASTM D 4643, respectively). The results are presented in Figures 3 and 4.

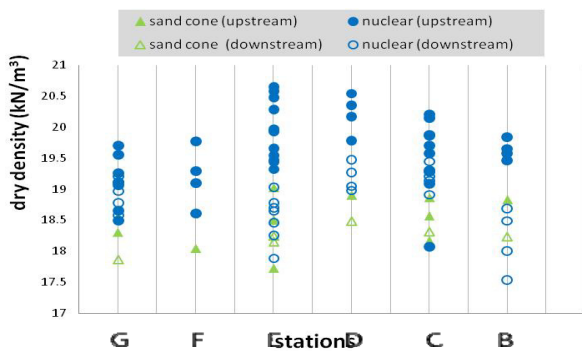


Figure 3. Dry density results.

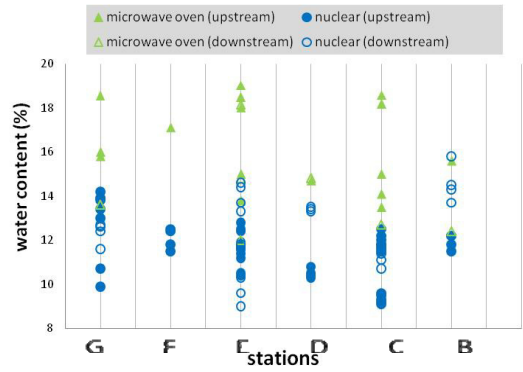


Figure 4. Water content results.

The dry densities results obtained by the nuclear gauge device are generally larger than those obtained by the sand cone device. The water content results determined with the nuclear gauge device are generally smaller than those obtained by the microwave oven device, especially on the upstream shell.

2.2.2 P-FWD testing

The used Prima 100 P-FWD device consists of four major parts: the sensor body, loading plate, buffer system and sliding weight (Figure 5).

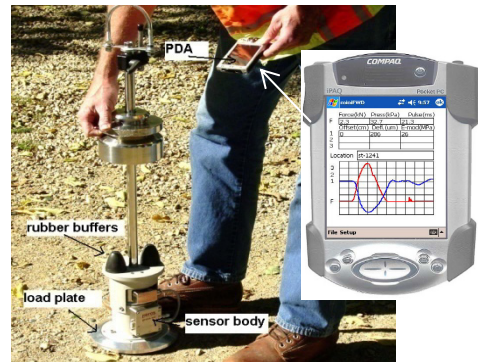


Figure 5. Prima 100 P-FWD device (Siekmeier, 2004).

The sensor body encloses a load cell and a central geophone. The geophone is spring mounted at the center of the load plate. The geophone measures the deflection of the superficial soil under an impact load. The Prima 100 allows the user to vary the drop height, weight, plate diameter and buffer configuration.

The weight and drop height can be varied to allow the user to increase or decrease the impact load. Additional drop weight increases the stress exerted by the plate. By changing the size of the loading plate diameter, the area over which the force is applied can be changed. This allows the user to change the stress imparted onto the sub-grade soil. The number of rubber buffers can be adjusted to alter the length of the load impact pulse.

The device measures both force and deflection. Data is transmitted to a hand-held computer (PDA) in conjunction with a Bluetooth device. The software enables to choose the test setup and to visualize and save the test results. Displayed results include time histories and peak values of load and deflection.

The peak values of load and deflection are employed in the software for calculating the elastic stiffness modulus,  $E_{PFWD}$ . The equation used to determine  $E_{PFWD}$  is similar to the one used to calculate the surface modulus of a layered material, assuming a uniform Poisson's ratio and constant loading, known as the Boussinesq equation:

$$E_{PFWD} = \frac{f(1-\nu)^2 \sigma R}{\delta_c} \quad (1)$$

where  $f$  is stress distribution factor, assumed 2.0 (flexible plate),  $\nu$  the Poisson's ratio, assumed 0.35 (coarse grained soil),  $\sigma$  the (peak) impact stress under loading plate (kPa),  $R$  the radius of P-FWD loading plate (150 mm) and  $\delta_c$  the (1<sup>st</sup> peak) center P-FWD deflection ( $\mu$ m).

Reported in Tables 2 and 3 are the mean and coefficient of variation (COV) of the  $E_{PFWD}$  at each location obtained from different drop weights (10 and 15 kgf) and different drop heights (0.8 and 0.4 m).

During the initial testing, a 300 mm diameter loading plate, two buffers, a 15 kg falling mass and a 0.8 m drop height were used. This configuration caused the apparatus to move after impact. It was observed that this affected the accuracy of the deflection measurement. Then, the configuration was changed to a 10 kg falling mass and a 0.4 m drop height. This reduced the shaking and moving of the apparatus during testing.

Table 2.  $E_{PFWD}$  values (upstream shell)

Identification		Drop		$E_{PFWD}$	
Location	Station	Weight (kgf)	Height (m)	Mean (MPa)	COV (%)
B 1000	U	15	0.8	39.5	1.31
	D			37.2	2.78
	LM			36.8	1.67
	RM			37.6	1.28
C 999	U	15	0.8	67.8	3.02
	D			51.9	3.53
	LM			60.2	2.99
	RM			61.3	4.51
C 1010	U	10	0.4	15.6	3.42
	D			16.5	4.95
	LM			15.3	4.08
	RM			14.7	5.65
C 1024	U	10	0.4	31.5	2.06
	D			23.7	0.96
	LM			33.4	2.21
	RM			36.4	3.31
D 1011	U	10	0.4	18.9	3.72
	D			16.4	3.33
	LM			15.1	6.95
	RM			16.2	2.53
E 1009	U	10	0.8	27.3	1.66
	D			31.2	4.04
	LM			52.6	6.81
	RM			43.7	2.89
	U	10	0.4	9.7	0.97
	D			12.5	2.39
	LM			-	-
	RM			-	-
E 1020	U	10	0.4	16.3	3.15
	D			12.2	1.36
	LM			15.9	3.16
	RM			15.2	2.84
E 1006	U	10	0.8	15.7	1.71
	D			30.1	1.68
	LM			30.3	3.51
	RM			31.1	0.93
F 1007	U	10	0.8	30.5	8.9
	D			33.1	1.04
	LM			31.8	1.41
	RM			31.3	1.63
G 1008	U	10	0.8	31.5	1.58
	D			27.8	1.10
	LM			32.1	6.2
	RM			40.5	2.64
G 1019	U	10	0.4	42.3	2.73
	D			13.0	0.57
	LM			12.2	2.65
	RM			11.8	3.22
				15.0	3.17

Table 3.  $E_{PFWD}$  values (downstream shell)

Identification		Drop		$E_{PFWD}$	
Location	Station	Weight (kgf)	Height (m)	Mean (MPa)	COV (%)
B 1012	U	10	0.4	19.4	1.75
	D			28.2	2.80
	LM			28.2	3.79
	RM			26.1	2.80
C 1013	U	10	0.4	35.6	1.37
	D			36.7	1.21
	LM			38.1	5.46
	RM			34.1	2.26
D 1001	U	15	0.8	41.2	4.71
	D			43.4	1.07
	LM			37.4	2.16
	RM			37.8	1.84
E 1002	U	15	0.8	36.1	1.20
	D			40.3	2.96
	LM			33.2	3.24
	RM			39.5	3.83
E 1026	U	10	0.4	26.7	5.57
	D			24.6	4.24
	LM			43.2	1.2
	RM			21.4	7.29
G 1027	U	10	0.4	26.7	5.70
	D			28.1	2.37
	LM			28.0	5.45
	RM			24.7	2.67

Figure 6 depicts the variation of the COV of each location with its corresponding average  $E_{PFWD}$ . Range of observed COV is relatively small, 0.57% to 8.9%, and decrease to 0.57% to 7.3% when 10 kg falling mass and a 0.4 m drop height were used. Accordingly, a decision was made to disregard locations B 1000, C999, E 1006, E 1007, D 1001 and E 1002 from the database of this study.

Upstream shell

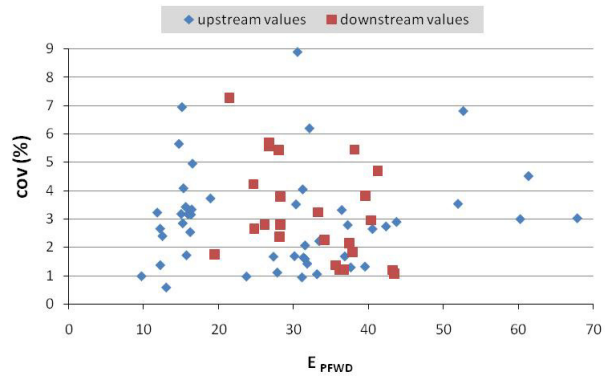


Figure 6. Repeatability of  $E_{PFWD}$ .

As can be seen in Figure 7 the 1<sup>st</sup> peak deflection of the loading plate is out of phase (in time) with the maximum applied contact stress. What it amounts to is that the use of conventional static load theory for interpretation of dynamic deflection is inconsistent, so it was decided to undertake a dynamic analysis.

Several researchers, such as Mamlouk (1987) and Uzan (1994), have investigated the limitations of static methods and underline the need for a consistent dynamic analysis of measured deflections.

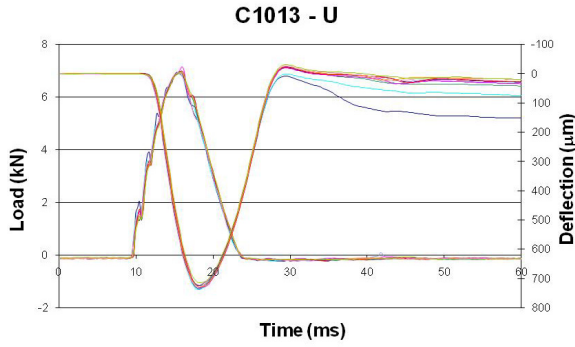


Figure 7. Load pulse and corresponding deflection curves (C 1013 location, U station).

### 3 DYNAMIC ANALYSIS

In general, the soil dynamic analysis (for nearly incompressible soils) is based on modeling the impact of a rigid weight on a simple spring-dashpot model. The contact force ( $F$ ), imposed on the soil by the falling weight, is theoretically equal to the sum of the reaction forces exerted by the spring and the dashpot (Voigt-Kelvin model):

$$C \dot{u} + K u = F \tag{2}$$

where  $u$  is the displacement,  $\dot{u}$  is the first derivative of  $u$  over time, and  $K$  and  $C$  are the characteristic parameters of the spring (stiffness) and the dashpot (damping).

The equation (2) was implemented parametrically to predict the load-deflection response of the soil at the point of falling weight impact, using a Simulink/Matlab tool. This parametric analysis was essential to check the general validity of equation (2) for the P-FWD results and for providing a simple relationship between the dynamic stiffness modulus ( $E_{dyn}$ ) of the soil in terms of maximum deflection and contact force at the point of weight impact, i.e.,  $K$ .

The results (Figure 8) are very satisfactory and the simulation is much faster than with the finite element method.

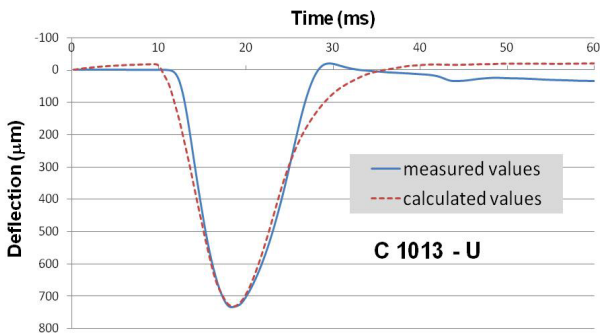


Figure 8. Comparison between calculated and measured values of deflection curve (5<sup>th</sup> drop at C 1013 location, U station).

For a circular loading surface on uniform and isotropic half-space, one reaches to the following expression for the  $E_{dyn}$ :

$$E_{dyn} = \frac{1 - \nu^2}{2 k_v R} K \tag{3}$$

where  $k_v$  is a dynamic spring coefficient (dependent of the frequency) and  $R$  is the radius of the loading plate.

### 4 CORRELATION BETWEEN K, IN SITU WATER CONTENT AND DRY UNIT WEIGHT

To check the feasibility of P-FWD for the purpose of compaction control, the correlation between  $K$ , in situ water content and dry unit weight variations were verified along the different locations (Figure 9).

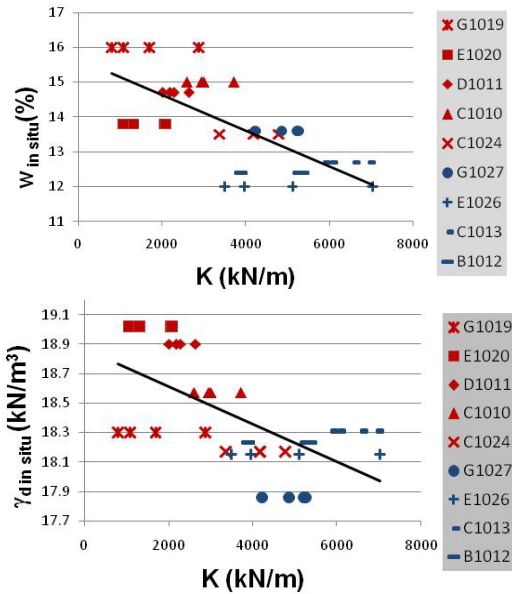


Figure 9. Correlation between  $K$ , in situ water content ( $w_{in\ situ}$ ) and dry unit weight ( $\gamma_{d\ in\ situ}$ ).

As expected,  $K$  decreases with water content, but with a significant dispersion. In terms of dry unit weight, the results show that  $K$  also decreases, what was not expected. It seems that the water content effect on the stiffness is more pronounced than the dry unit weight.

### 5 CONCLUSIONS

The current research leads to the following conclusions and remarks:

- Prima test results are significantly affected by the shaking and moving of the apparatus during testing;
- Field test results are conclusive to suggest a good repeatability of  $E_{PFWD}$  values;
- The static approach to the interpretation of the P-FWD data have limitations which led to the need for a dynamic analysis of measured deflections;
- The Kelvin-Voigt model provides a good agreement with the P-FWD deflection results;
- The suitability of P-FWD tests for the purpose of compaction control needs further research.

### REFERENCES

Siekmeier, J., 2004. Continuous Compaction Control and Other Innovative Field Tests, FHWA Intelligent Compaction Strategic Forum, NCAT, Auburn, Alabama, USA, December 14-15.  
 Mamlouk, M. S., 1987. Dynamic analysis of multilayered pavement structures-Theory significance and verification. Proceedings of the 6th International Conference on Structural Design of Asphalt Pavements, Ann Arbor, Michigan, July 13-17.  
 Uzan, J., 1994. Advanced back-calculating techniques. Nondestructive Testing of Pavements and Back-calculation of moduli, ASTM 1198 pp. 3-37.